Numerical study on optimization of heat transfer through a micro channel

1Deepesh Tyagi, 2Prof. Ashish Muchrikar
1M.Tech Scholar, 2Professor & Head Department of Mechanical Engineering
1Corporate Institute of Science and Technology, Bhopal, India,
2Corporate Institute of Science and Technology, Bhopal, India

***Abstract* - the presented study deals with slug flow in a micro channel with wall heat flux boundary condition. A cfd analysis has been carried out on a 2-dimensional axisymmetric model with three different heat flux value and nusselt no. is plotted. Also the taylor bubble formed is analyzed by plotting the air volume fraction to represent the bubble. The three heat flux values are 10000 W/m2, 20000 W/m2 and 30000 W/m2 which corresponds to the average nusselt number 17.255, 17.377 and 16.493 respectively which shows that at first nusselt number increases by increasing the heat flux at wall and then it decreases and hence maximum heat transfer occurs at 20000 W/m2 heat flux. The local wall temperature along the length and local nusselt number along the wall is also plotted in analysis. The results obtained in the study is validated against the existing work and found in good agreement with the existing data**

***keywords* - computational fluid dynamics, micro channel, local nusselt number, air volume fraction, slug flow, heat flux**

I. INTRODUCTION

With the rapid development of micro devices and micro systems in the last two decades, it has became very important to understand the effects of fluid flow properties and heat transfer mechanisms in mini channels and micro channels. The development in the Micro-Electro- Mechanical Systems (MEMS) and Micro-Flow Devices (MFD) requires heat removal systems that are equally small. Progresses in biomedical and genetic engineering entail controlled fluid carriage and its detailed thermal control in channels of several micrometer dimensions. Micro channels are applicable in a range of devices integrating particular phase liquid stream. The early applications involved micro-machined maneuvers such as micro-pumps, micro-valves, and microsensors. The concept was coined by a push in the organic and life sciences with a prerequisite of scrutinizing biological constituents such as proteins, DNA, cells, and chemical reagents. A correct understanding of carriage phenomena in these microscale structures is therefore vital for their design and operation.

It is indispensable for the design of micro conduit heat sinks to be competent to correctly foresee the transport stuffs under altered flow and thermal environments, especially in the entering region (i.e. when the flow is in the developing laminar region). Moreover, it is of prime importance to apply correct thermal boundary conditions to estimate the accurate heat transfer effects from a system.

Gas – Liquid flow pattern : Two-phase (liquid-gas) stream inside a conduit is a intricate phenomenon which is uttered by various contending forces such as shear stress, capillarity, gravity and momentum. Such complex situations gets even extra intricate by the continuous crusade of the phase boundaries which introduces a disrupting effect into the flows and causes the changes of temporal and spatial distributions of the phases. Because of the complex characteristics of the liquid and gas flow, the two-phase flow is often classified as a unique flow pattern and presented in a flow-pattern (sometime denotes "flow-regime") map. Therefore, the correlations for the pressure drop and heat transfer for two-phase flows should be flow regime-specific for accurate extrapolation of behaviors of two-phase systems.

Explanation of two-phase flow arrangements is frequently subjective and there is no precise quantitative technique to define and classify the stream shapes. The following descriptions are based on the most widely accepted classifications of the gas-liquid two-phase flows in a horizontal tube:

- Stratified flow : The gas molecules drifts alongside the upper part of the horizontal channel whereas the liquid trips alongside the bottom with no significant interfacial waves.. As can be seen in Fig. 1(a), this fluid current has the simplest arrangement of all the horizontal stream shapes and sometimes denoted as "stratified smooth" stream pattern.
- Wavy flow : Increment in gas velocity in stratified streams, ripples the shear forces of the gas stream over the liquid, cause the gas-liquid boundary in the development of waves. The surfs climb up the sides of the conduit but frequently do not tad the top side of the conduit wall and the liquid film at the bottommost of the conduit starts to expanse thin [Fig. 1(b)]. This flow is often discussed as "stratified wavy" stream pattern.
- Plug flow : As shown in from Fig. 1(c), elongated gas bubbles in bullet-shaped and liquid plugs appear alternatively on top of the pipe. The diameter of the extended bubbles are lesser than the pipe diameter which permits for a continuous liquid phase to look on the bottom of the pipeline.
- Slug flow : With large amplitude wave or squishes of liquid, eventually, the waves build up and spread the upper wall of the pipe to form liquid slugs. These liquid slugs are then transported at the higher velocity of the gas [see Fig 1(d)]. Unlike the plug flow, in which the elongated bubbles are transported by the liquid phase, in the slug flow,

the liquid slugs are carried by the faster moving gas flow. It is worth mentioning that the slug flow regime is highly undesirable in practical application.

- Annular flow : This flow is momentum-dominant and occurs at relatively high gas flow rates. As shown in Fig. 1(e), the liquid shapes a constant flick round the border of the tube wall and gas steams as a inner core and entrains small precipitations of liquid disseminated in the form of mist. Small bubbles of gas may also be entrained in the liquid flick.
- Bubbly flow : This flow regime takes place at very high liquid flow rates. As shown in Fig. 1(f), gas bubbles are dispersed in a continuous liquid phase. The bubbles are relatively small in comparison with the tube diameter and tend to rise to the top of the pipe due to buoyancy force. However, when the liquid velocity is larger, shear forces are prevailing and unchanging dispersal of bubbles follow in the pipe. This flow regime is really a separate category. (a) to (e) can be obtained by simply increasing superficial velocity of gas at the same superficial velocity of liquid, which is just the opposite of how the bubbly flow is obtained.

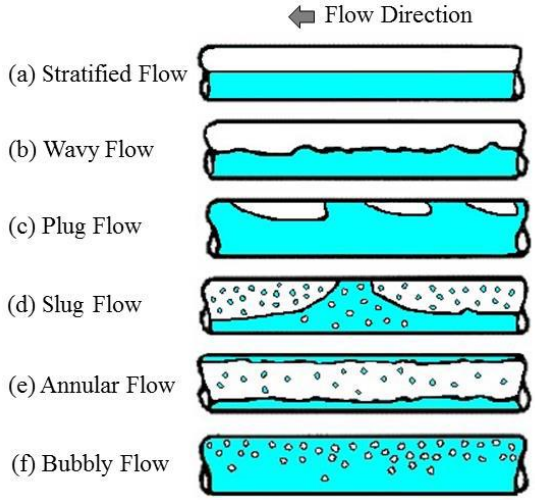

Figure 01 : Representative two-phase flow patterns in a horizontal pipe.

II. LITERATURE REVIEW

Triplett et al. [1] Two-phase flow regimes in micro channels have been investigated experimentally With the exception of stratified flow, the major flow patterns that are common in macro- channels happen in micro conduits, though firm stream outline details may be diverse from those in big channels. Fig. 2 displays the regularly cited stream-regime map of Triplett which was settled for air–water two-phase flow in a horizontal circular conduit of 1.45 mm inner diameter in gas superficial velocity(UGS) versus liquid apparent velocity(ULS) coordinates .Five main flow regimes were identified, as shown in Fig. 1, namely bubbly, slug, churn, slug-annular and annular flow.

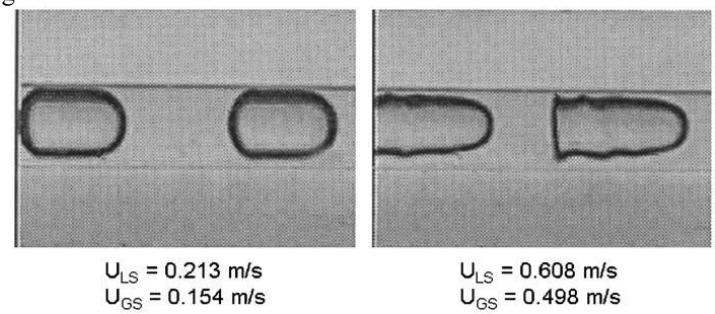

Figure 02 : Representative photograph of Taylor or slug flow in a 1.1mm circular micro channel as observed by Triplett et al.(1999).

Barajas and Panton et al. [2] determined the flow patterns visually in 1.6mm horizontal channels of four different materials having different contact angles for an air–water system. Lump flow was similar to Taylor stream as defined here, while slug stream was defined as a stream pattern holding intermittent slugs of liquid obstructive the entire canal cross-section.

Zhao and Bi et al. [3] explored the air–water two-phase stream shapes in vertical symmetrical triangular section channels with hydraulic diameters of 2.89, 1.44 and 0.87mm. It was noted that, in the channel of smallest dimension, a capillary bubbly flow pattern, regarded as a train of ellipsoidal-shaped bubbles crossing al- most the entire channel cross-section, led to the side-walls being incompletely dry at truncated liquid stream rates.

Serizawa et al. [4] deliberate air–water two-phase flow in curved tubes of 20–100 µm and detected different stream patterns, such as detached bubbly flow, gas slug stream, liquid ring flow, liquid lump stream, skewered barbecue (Yakitori) shaped flow, annular stream and rivulet flow. They also jagged out that arid and wet zones occurred between the gas slug and conduit wall at small velocities.

Cubaud and Ho et al. [5] performed experimental inquiries of gas–liquid two phase stream in 200and500 µm square-section microchannels. In the experiments, de wetting was observed in two flow-regimes, named wedge stream and dry flow. In

wedge stream they state: "For a partly wetting system, as a function of the gurgle velocity, bubbles can arid out the center of the conduit crafting triple lines (liquid/gas/solid).The liquid flick amongst the gas and the of the conduit can be reflected as static, while liquid streams in the corner." This partly dry-out of the conduit walls is comparable to that observed by Zhao and Bi (2001) in triangular micro conduits. The dry flow happens when the homogeneous void fraction is additional than 0.995 and the liquid stream is limited to that of the conduit.

Van Baten and Krishna et al. [6] simulated the stream in the liquid flow field around the bubble and also explored mass diffusion from Taylor bubbles to the liquid phase. They exhibited that a very fine matrix (cell size smaller than 1 μm for a conduit of 3mm diameter) was essential to arrest the steep concentration gradients nearby the bubble exterior and in the fluid flick.

Giavedoni and Saita et al. [7] investigated mathematically the liquid stream field in the primary front and the rear part of a long bubble disjointedly by using a finite volume method which permitted the bubble boundary to move.

Kreutzer et al. [8] also used a finite element method to mimic the flow around the bubble consenting the bubble boundary to move.

Taha and Cui [9] considered the stream of Taylor bubbles in a vertical tube-like membrane of diameter 19mm using different models: VOF, Eulerian two fluid, and a strategy that applied a solution-adapted distributed- phase length-scale, using ANSYS CFX-5.6.

Taha and Cui [10] showed Taylor stream in a erect capillary for a two-dimensional, axisymmetric geometry using Fluent. A computational domain of length of 11 diameters having matrix size 26 * 280 with the grid being developed near the wall. The stream field was explained in a allusion border moving with the bubble. A constant velocity was quantified at the inlet and outstream boundary condition was used at the outlet.

Qian and Lawal [11] applied Fluent to simulate Taylor bubble development in a T-junction micro conduit for a 2-dimensional planar geometry with a cross-sectional size fluctuating from 0.25 to 3mm. The gas and liquid were nourished from the two unlike legs of the T- junction. The effect of inlet configuration, gas and liquid stream rates and belongings on the slug length was considered. The length of the stream domain was 60 tube diameters and the computational mesh contained only 6600 cells which is too coarse to capture the details of the stream.

Fukagata et al. [12] modelled 2-dimensional, axisymmetric, periodic Taylor bubble stream and heat flow (without phase change) in a 20 μm tube using the level set approach. The void fraction, pressure gradient, bubble period and wall heat flux were cast-off as input stricture. The bubble profile and the stream arena round it were considered and used to define the gas and liquid apparent velocities and the two-phase frictional multiplier. They equated their outcomes with the experimental figures of Serizawa et al. (2002) and found judicious covenant between the two. They also perceived that the bubble retro has a large influence on the stream decoration.

He et al. [13] examined 2-dimensional axisymmetric numerical simulations of gas–liquid two phase stream in a conduit having a radius of 10 μm and a length of 40 μm using the phase-field approach. A periodic boundary condition with stated pressure drop was smeared in the streamwise direction. A square grid was used with 32 elements in the radial direction. Void fraction, pressure drop and initial velocity (either zero or a parabolic velocity profile) and an assumed bubble outline were recycled as the input. The final bubble outline and the apparent velocities of the gas and liquid were considered in the simulation.

Yu et al. [14] premeditated gas–liquid stream in rectangular micro conduits experimentally and mathematically. The numerical study was carried out using the Lattice–Boltzmann method. The liquid flick was successfully apprehended at capillary numbers (based on liquid properties) of 0.03 or above. However, the flick could not be taken successfully at lower values of capillary number It was distinguished that this botch in capturing the liquid flick could be accredited to the limited tenacity of the simulations.

Kumar et al. [15] premeditated Taylor flow mathematically in curved micro conduits of diameters fluctuating from 0.25 to 3mm. A mesh- individuality revision was carried out for four dissimilar mesh densities. The reading showed that the gas–liquid boundary became shrill as the mesh was sophisticated, which is a straight consequence of using a re- fined mesh in the streamwise direction. Still, the liquid flick on the surface was not engaged by even the finest mesh used, because the radial mesh was not refined adequately. The effect of inlet geometry, conduit diameter, curvature ratio, inlet volume fraction, surface tension, liquid viscosity and wall contact angle on slug length was studied.

III. OBJECTIVE

The objective of the present study is to perform a two-dimensional axisymmetric CFD analysis of a slug flow in a microchannel involving heat transfer to observe the suitability of its application.

- To validate the CFD result data of the present analysis with existing work of slug flow.
- To plot a Nusselt No. curve for different wall heat flux condition so as to measure the effectiveness of the microchannel in a range of heat flux value.
- To visualize the different properties in the flow field.
- To observe the pressure exerted on the wall due to bubble formation.
- To observe the time of first bubble passing out of the pipe as it is difficult to measure these values analytically in a microchannel.

IV. METHODOLOGY

In the present work a CAD model of micro conduit is created using Design modular designing software. For creating the model dimension were considered base paper data. Computational fluid dynamic analysis have been performed for all four models at different wall heat flux are as follow :

- No heat flux at outer wall of micro channel
- 10000 w/m^2 heat flux at outer wall of micro channel
- 20000 w/m^2 heat flux at outer wall of micro channel
- 30000 w/m^2 heat flux at outer wall of micro channel

Governing Equations

The equation for preservation of mass,

$$\frac{\partial \rho}{\partial t} + \nabla.(\rho\,\vec{v}) = S_m$$

Where S_m= mass included to the continuous phase or any handler sources.

For 2D axisymmetric model, the continuity equation is given by

$$\frac{\partial \rho}{\partial t} + \frac{\partial}{\partial x}(\rho v_x) + \frac{\partial}{\partial r}(\rho v_r) + \frac{\rho v_r}{r} = S_m$$

Where x being the axial coordinate, r being the circular coordinate, v_x is the axial velocity, and v_r is the radial velocity.

Momentum Conservation Equations

Conservation of momentum in an inertial reference frame is described by

$$\frac{\partial}{\partial t}(\rho\vec{v}) + \nabla.(\rho\vec{v}\vec{v}) = -\nabla p + \nabla.(\bar{\bar{\tau}}) + \rho\vec{g} + \vec{F}$$

$$\bar{\bar{\tau}} = \mu\left[(\nabla\vec{v} + \nabla\vec{v}^{\mathrm{T}}) - \frac{2}{3}\nabla.\vec{v}I\right]$$

Energy Equation

$$\frac{\partial}{\partial t}\sum_{k=1}^{n}(\alpha_k\rho_k E_k) + \nabla.\sum_{k=1}^{n}(\alpha_k\vec{v}_k(\rho_k E_k + p)) = \nabla.\left(k_{eff}\nabla T\right) + S_E$$

k* −∈ *model

The turbulence kinetic energy, k, and its rate of dissipation, ∈, are obtained from the following transport equations:

$$\frac{\partial}{\partial t}(\rho k) + \frac{\partial}{\partial x_i}(\rho k v_i) = \frac{\partial}{\partial x_j}\left[\left(\mu + \frac{\mu_t}{\sigma_k}\right)\frac{\partial k}{\partial x_j}\right] + G_k + G_b - \rho \in - Y_M + S_k$$

and

$$\frac{\partial}{\partial t}(\rho \in) + \frac{\partial}{\partial x_i}(\rho \in v_i) = \frac{\partial}{\partial x_j}\left[\left(\mu + \frac{\mu_t}{\sigma_\in}\right)\frac{\partial \in}{\partial x_j}\right] + C_{1\in}\frac{\in}{k}(G_k + C_{3\in}G_b) - C_{2\in}\rho\frac{\in^2}{k} + S_\in$$

In addition mixture model is used to track multiphase flow.

CAD geometry of microchannel: Two dimensional CAD model of micro channel is created using the design modular software with dimension from the model used in the work of Rghvendra Gupta et al.

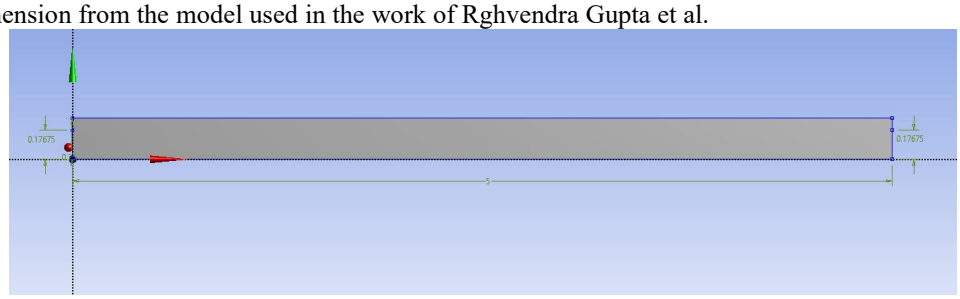

Figure 03: Two dimensional CAD geometry of model

Studied micro conduit: A micro conduit with simple geometry is used in the present study (Fig. 3) to clarify the effect of changing the wall heat flux. The micro main specifications are given in Table 1.

Table 01: micro channel specifications.

Dimensions	Value
length of channel	5mm
Dia of channel	0.5mm
Dia of first phase at inlet	0.3535mm

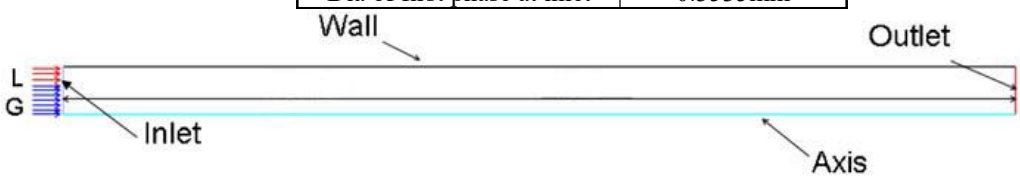

Figure 04: View of the selected channel simplified view.

Meshing: After completing the CAD geometry of model of micro channel is imported in ANSYS mechanical for further computational fluid dynamics analysis where next step is meshing. The total number of nodes generated for this model is 51051 and total number of Elements is 50000. Types of elements used are quadrilateral which is square in shape with four nodes on each element.

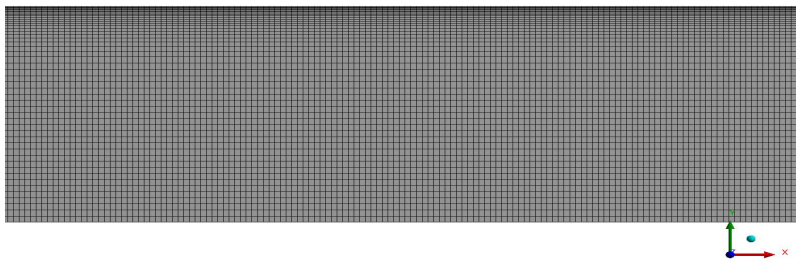

Figure 05: Meshing of CAD model zoomed view.

Boundary conditions are assigned to create a virtual environment of the real life working of the system. The boundary conditions for simulation of centrifugal pump are explained below :

- Define the solver settings as pressure based transient and enable gravity option in y direction with the value of -9.81 m/s^2.
- Working fluid is water and air with density 1.22 kg/m^3 for air and 998.2kg/m^3 for water, viscosity 1.789 e-05 kg/m-s for air and 0.001003 kg/m-s for water, Thermal conductivity 0.24 W/m^2-K.
- Set viscose model laminar flow.
- Turn on multiphase model and select mixture model for simulating slug flow.
- Surface tension coefficient between air and water is 0.072n/m.
- Air inlet velocity is 0.49 m/sec and for water inlet velocity is 0.51
- Set the heat flux at wall as per cases in boundary conditions.
- For the operating condition the operating pressure needs to be set as 101325pa.
- Under Discretization, select scheme for SIMPLE, and QUICK for Momentum and Energy equation
- The Fluent solver is used for CFD analysis.

V. RESULTS.

Validation : The geometrical stricture for micro channel is considered from from the model used in the work of Rghvendra Gupta et al. the working fluid used in simulation is water liquid and air having properties such as density 988.2 Kg/m3 for water liquid, viscosity 0.001003 kg/m-s for water liquid, 1.225 Kg/m3 and 1.7894e-5 kg/m-s for air . Types of elements used are quadrilateral which is square in shape with four nodes on each element.

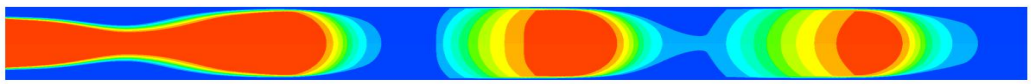

Figure 06: present study result contour of volume fraction that shows bubble formation at time 8.5 ms. The liquid is shown in blue and the gas in red.

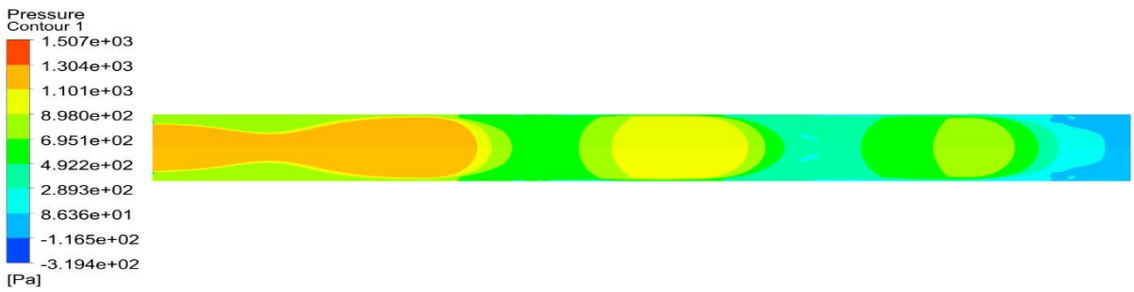

Figure 07: Present study pressure contour plot

Computation fluid dynamics analysis for base models : Computational fluid dynamics analysis of micro channel for base model at inlet velocity 0.49 m/s for air and 0.51 m/s for water is done. Volume fraction and pressure distribution for validation cases shown by contour diagram previously and now pressure variation across channel is shown in form of graph:

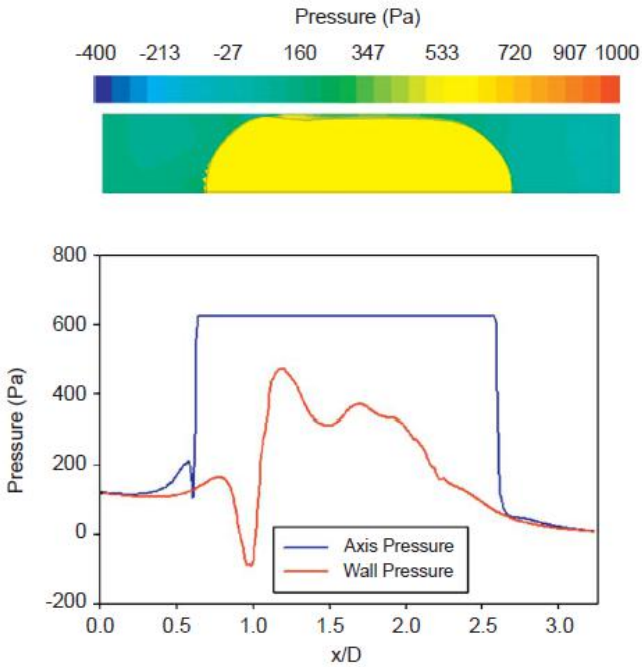

Figure 08 : Base paper variation of pressure on the axis axis and wall for a unit bubble pipe

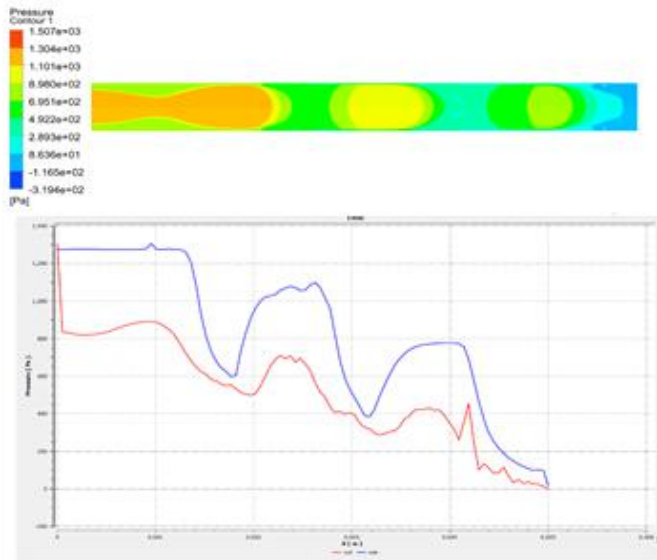

Figure 09: Present study variation of pressure on the and wall for whole

After the validation of base model some other cases of micro channel slug have been used for computational fluid dynamics analysis to investigate thermal effect in slug flow in micro channels. In the present work it has been try to investigate micro channel slug flow at different constant heat flux at wall with constant inlet and constant model of pipe.

Results for CFD analysis of micro channel slug flow at different hat flux is shown: After performing computational fluid dynamic analyses with absolute velocity formulation using pressure based solver. Different parameter distribution inside the micro channel with velocity 0.49 m/s for air and 0.51 m/s for water. After performing computational fluid dynamic analyses with absolute velocity formulation using pressure based solver. Different parameter distribution inside the micro channel with velocity 0.49 m/s for air and 0.51 m/s for water is shown. The monitored results are shown in form of contour and graphs :

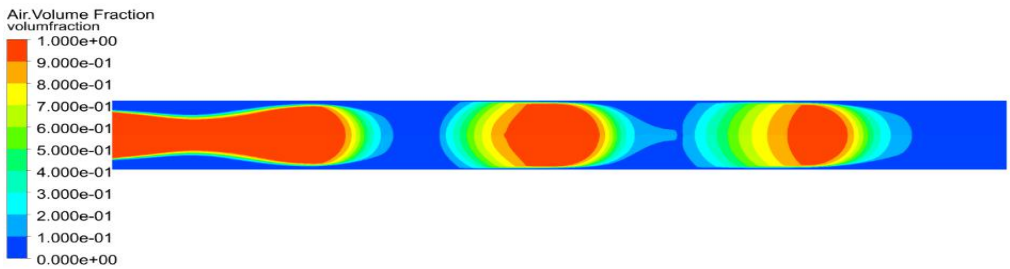

Figure 10 : Volume fraction contour for microchannel slug flow at 10000 w/m^2

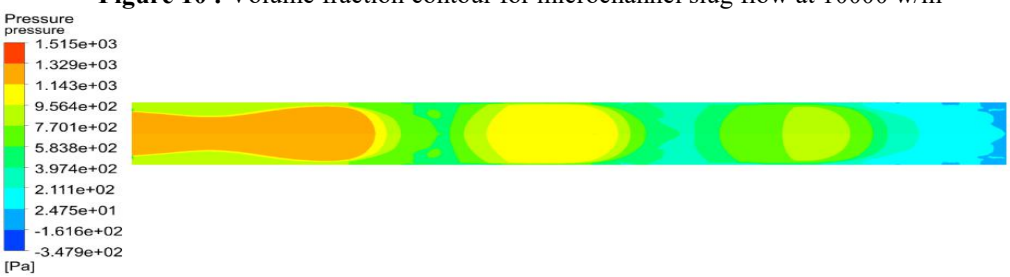

Figure 11 : Pressure contour for microchannel slug flow at 10000 w/m^2

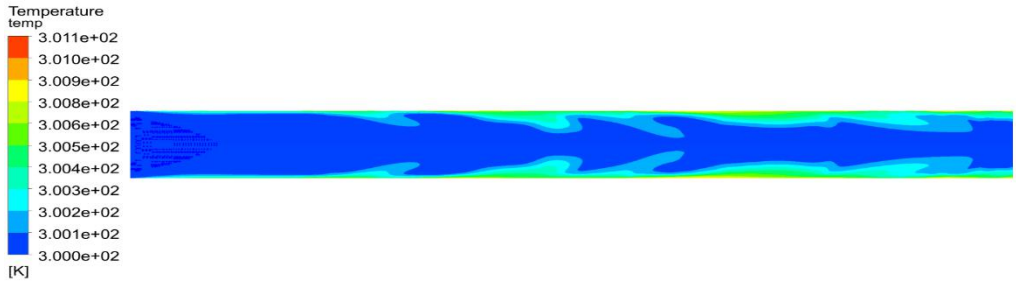

Figure 12 : Temperature contour for microchannel slug flow at 10000 w/m^2

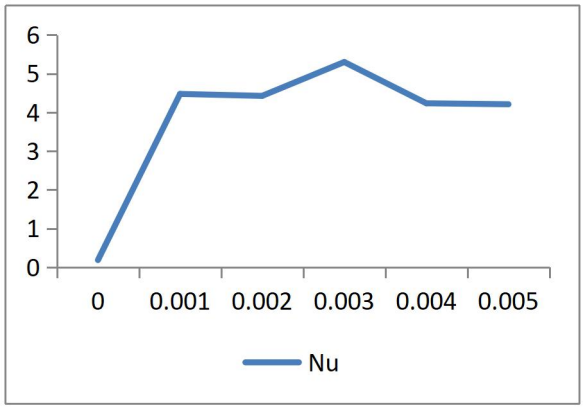

Figure 13 : Nusselt number variation across channel at 10000 w/m^2

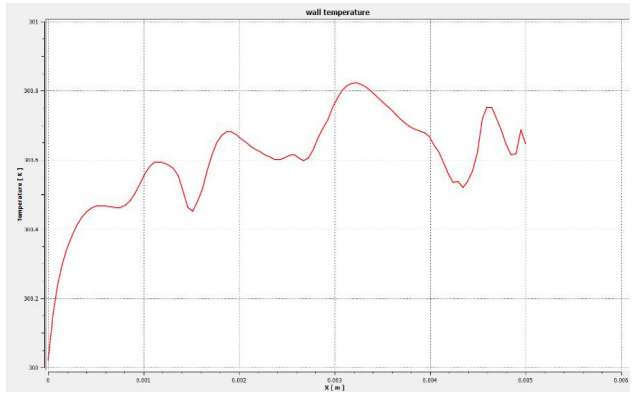

Figure 14 : Wall temperature plot for microchannel slug flow at 10000 w/m^2

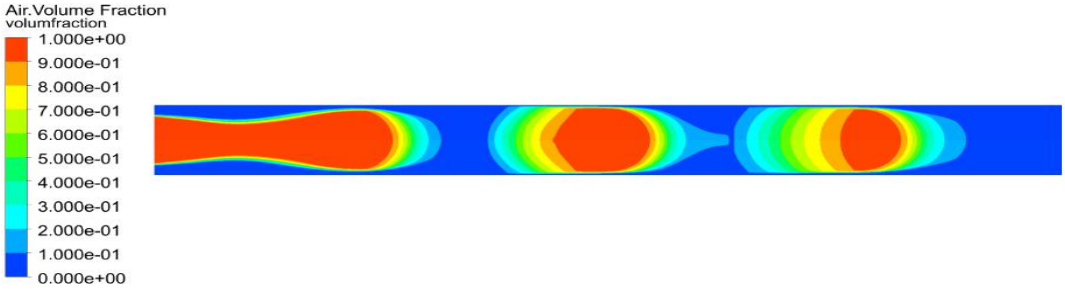

Figure 15 : Volume fraction contour for microchannel slug flow at 20000 w/m^2

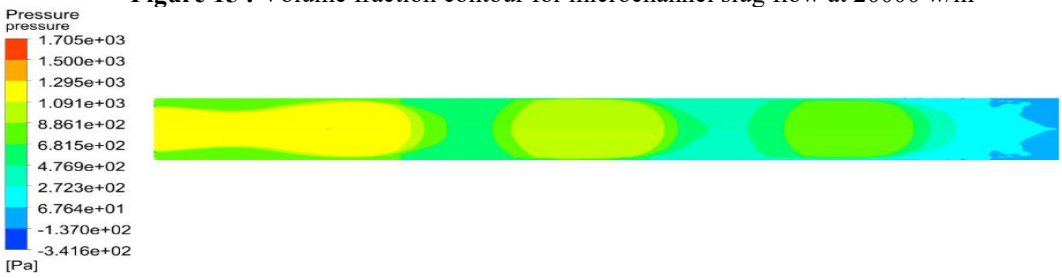

Figure 16 : Pressure contour for microchannel slug flow at 20000 w/m^2

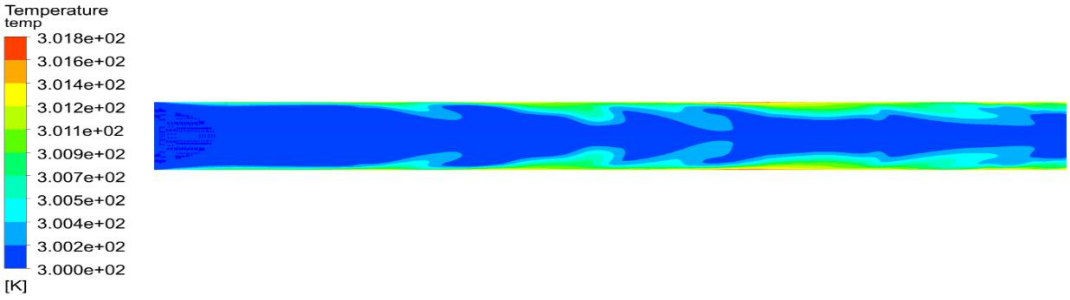

Figure 17 : Temperature contour for microchannel slug flow at 20000 w/m^2

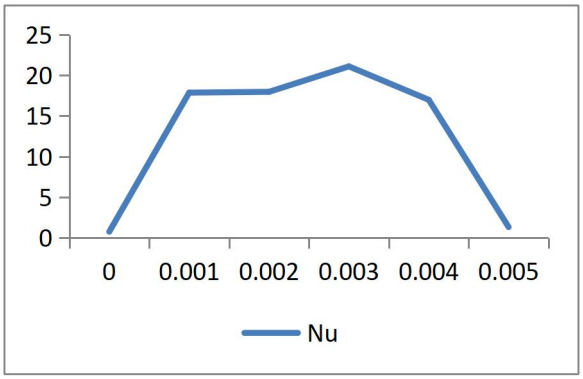

Figure 18 : Nusselt number variation across channel at 20000 w/m^2

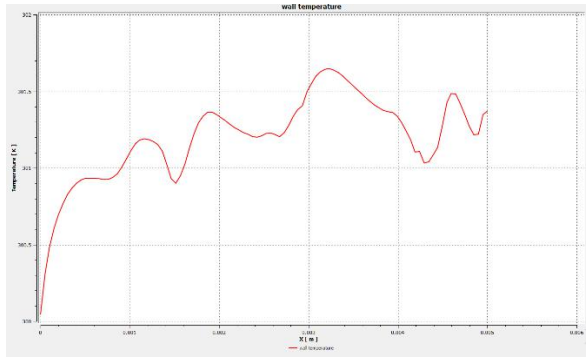

Figure 19: **W**all temperature plot for microchannel slug flow at 20000 w/m^2

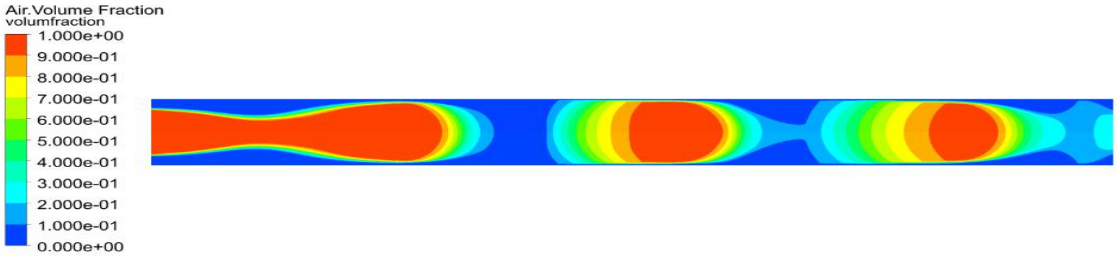

Figure 20 : Volume fraction contour for microchannel slug flow at 30000 w/m^2

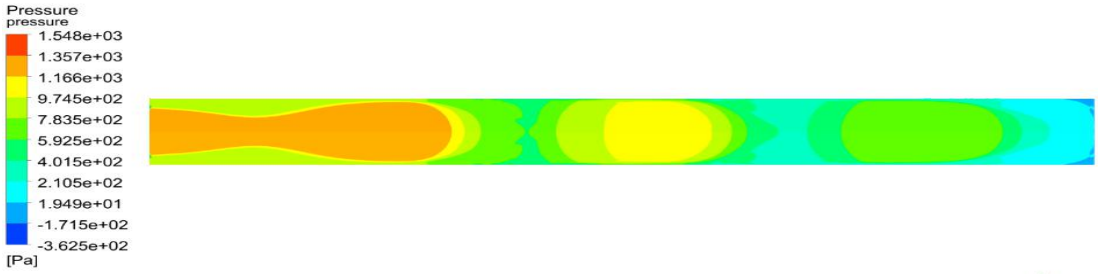

Figure 21 : Pressure contour for microchannel slug flow at 30000 w/m^2

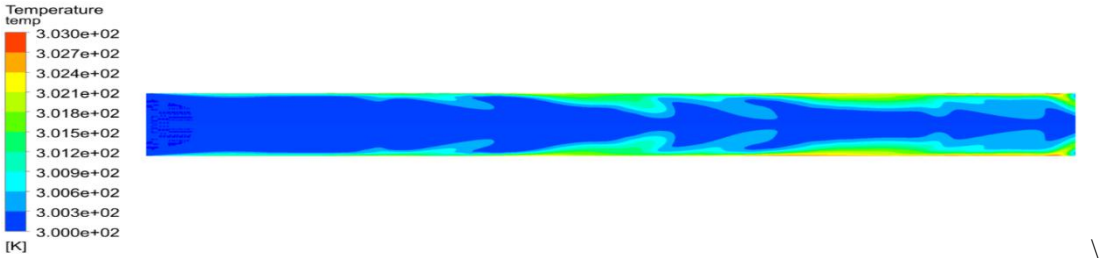

Figure 22 : Temperature contour for microchannel slug flow at 30000 w/m^2

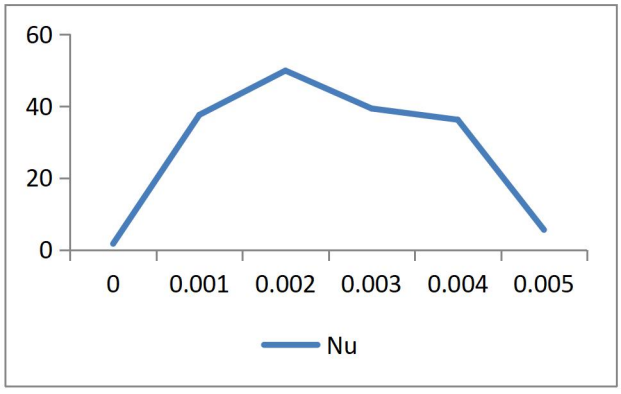

Figure 23 : Nusselt number variation across channel at 30000 w/m^2

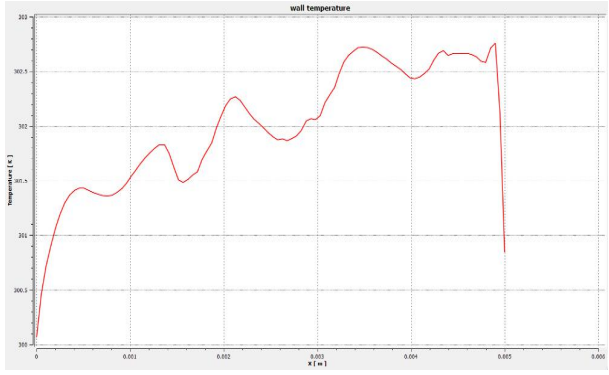

Figure 24: Wall temperature plot for microchannel slug flow at 30000 w/m^2

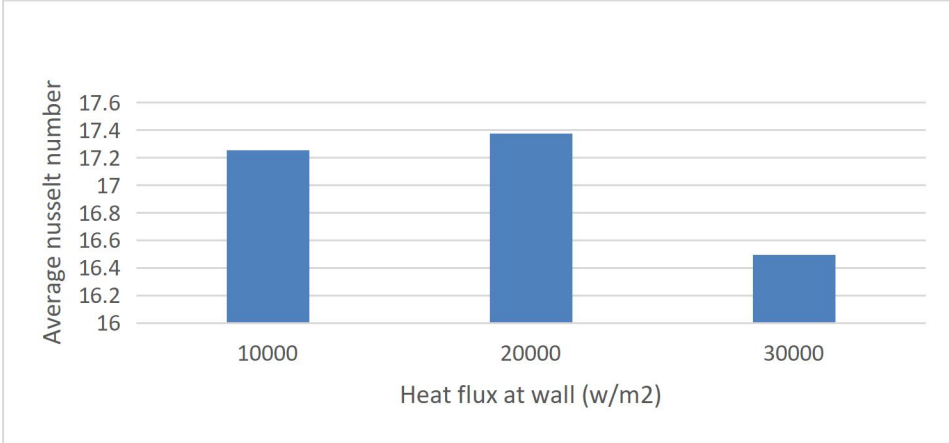

Figure 25 : Comparison of average nusselt number in all cases

VI. CONCLUSION

The results obtained is analysed for slug flow in a microchannel including the wall heat flux boundary conditions and Nusselt number is mainly checked for the suitability of application of microchannel in different heat flux condition and following conclusions were drawn:

1. The pressure plot alongside the length at centreline shows that as the bubble proceed alongside the length the pressure in bubble decreases which shows the size of bubble is slightly reduced. Pressure exerted on wall is also reduced as flow proceed alongside the length.
2. The first bubble coming out of the tube is at 8.5 ms.
3. The average Nusselt number for 10000 W/m2, 20000 W/m2 and 30000 W/m2 is 17.255, 17.377 and 16.493 respectively which shows that at first Nusselt number increases by increasing the heat flux at wall and then it decreases and hence maximum heat transfer occurs at 20000 W/m2 heat flux.
4. Maximum fluctuation in local wall temperature alongside length for 10000, 20000 and 30000 W/m2 heat flux is 0.9K, 1.6K and 2.7K respectively which shows that as we increase the heat flux value wall temperature increases.

REFERENCES

[1] Triplett, K.A., Ghiaasiaan, S.M.,Abdel-Khalik, S.I.,Sadowski, D.L., 1999. Gas–liquid two-phase flow in micro channels Part1: two-phase flow patterns. International Journal ofMultiphaseFlow25(3),377–394.

[2] Barajas, A.M., Panton, R.L., 1993. The effect of contact angle on two-phase flow in capillary tubes. International Journal of Multiphase Flow 19, 337–346.

[3] Zhao, T.S., Bi, Q.C., 2001. Co-current air–water two-phase flow patterns in vertical triangular microchannels. International Journal of Multiphase Flow 27 (5), 765–782.

[4] Serizawa, A., Feng, Z., Kawara, Z., 2002. Two-phase flow in microchannels. Experimental Thermal and Fluid Science 26 (6–7), 703–714.

[5] Cubaud, T., Ho, C.M., 2004. Transport of bubbles in square microchannels. Physics of Fluids 16 (12), 4575–4585.

[6] van Baten, J.M., Krishna, R., 2004. CFD simulations of mass transfer from Taylor bubbles rising in circular capillaries. Chemical Engineering Science 59 (12), 2535–2545.

[7] Giavedoni, M.D., Saita, F.A., 1997. The axisymmetric and plane cases of a gas phase steadily displacing a Newtonian liquid—a simultaneous solution of the governing equations. Physics of Fluids 9 (8), 2420–2428.

[8] Kreutzer, M.T., Kapteijn, F., Moulijn, J.A., Kleijn, C.R., Heiszwolf, J.J., 2005. Inertial and interfacial effects on pressure drop of Taylor flow in capillaries. A.I.Ch.E. Journal 51 (9), 2428–2440.

[9] Taha, T., Cui, Z.F., 2002. CFD modelling of gas-sparged ultrafiltration in tubular membranes. Journal of Membrane Science 210 (1), 13–27.

[10] Taha, T., Cui, Z.F., 2004. Hydrodynamics of slug flow inside capillaries. Chemical Engineering Science 59 (6), 1181–1190.

[11] Qian, D., Lawal, A., 2006. Numerical study on gas and liquid slugs for Taylor flow in a T-junction microchannel. Chemical Engineering Science 61 (23), 7609–7625.

[12] Fukagata, K., Kasagi, N., Ua-arayaporn, P., Himeno, T., 2007. Numerical simulation of gas–liquid two-phase flow and convective heat transfer in a micro tube. International Journal of Heat and Fluid Flow 28 (1), 72–82.

[13] He, Q., Fukagata, K., Kasagi, N., 2007. Numerical simulation of gas–liquid two-phase flow and heat transfer with dry-out in a micro tube. In: Proceedings: Sixth International Conference on Multiphase Flow, Leipzig, Germany.

[14] Yu, Z., Hemminger, O., Fan, L.-S., 2007. Experiment and lattice Boltzmann simulation of two-phase gas–liquid flows in microchannels. Chemical Engineering Science 62 (24), 7172–7183.

[15] Kumar, V., Vashisth, S., Hoarau, Y., Nigam, K.D.P., 2007. Slug flow in curved microreactors: hydrodynamic study. Chemical Engineering Science 62 (24), 7494–7504.